Available online at www.sciencedirect.com
ScienceDirect
Journal of Power Sources 159 (2006) 894–899
JOURNAL OF POWER SOURCES
www.elsevier.com/locate/jpowsour

Short communication

# A nanocomposite proton exchange membrane based on PVDF, poly(2-acrylamido-2-methyl propylene sulfonic acid), and nano-$Al_2O_3$ for direct methanol fuel cells

Juan Shen, Jingyu Xi, Wentao Zhu, Liquan Chen, Xinping Qiu *

*Key Lab of Organic Optoelectronics and Molecular Engineering, Department of Chemistry, Tsinghua University, Beijing 100084, China*

Received 26 October 2005; received in revised form 18 November 2005; accepted 23 November 2005
Available online 6 January 2006

**Abstract**

A proton exchange membrane based on poly(vinylidene fluoride) filled with nano-sized ceramic fillers and a kind of polymeric acid was prepared and characterized with FT-IR, TGA, and SEM. The membrane shows high and stable conductivity at room temperature. The role of the ceramic filler and the polymer acid in the enhancement of the proton productivity is discussed. Proton conductivities and methanol permeabilities of membranes with different contents of ceramic fillers were investigated. The ratio between the conductivity and methanol permeability shows the membranes with over 16 wt.% content of alumina fillers are the best membranes prepared in this work for use in a direct methanol fuel cell.


*Keywords:* PVDF; PAMPS; Proton exchange membrane; DMFC; Methanol permeability

## 1. Introduction

Proton exchange membranes (PEMs) play an important role in direct methanol fuel cells (DMFCs). The most widely used PEMs are perfluorosufonate membranes, like Nafion. These membranes have a high specific conductivity at room temperature, as well as good mechanical, chemical, and thermal stability. However, the cost and high methanol permeability are the main difficulties for using them in DMFCs [1]. In addition, the dehydration of the membranes at higher temperatures decreases their proton conductivity [2]. Therefore, much work has been devoted to modifications of Nafion membranes [3,4] and development of new PEMs [5–10] including composite membranes prepared by incorporating ceramic powders such as $SiO_2$ and $TiO_2$ into polymers and absorbing acid with a phase-inversion process. Nafion/silica hybrid membranes with various silica contents were prepared by incorporation via an in situ sol–gel reaction of TEOS. The results showed the methanol permeability was reduced with a high silica content [3,4]. But Tricoli and Nannetti [5] has reported that composite membranes formed of zeolite embedded in Nafion were inferior to the zeolite-free recast Nafion membranes considering the performance in both ion conductivity and transport selectivity. Polyvinyl alcohol (PVA) membranes containing mordenite have also been prepared with higher selectivity than Nafion [6] and the authors suggested the polymer used should be less conductive to take advantage of the selectivity of the particles. Composite membranes based on zeolite dispersed in a PTFE matrix were prepared and showed higher proton conductivities at a higher zeolite content [7]. Peled et al. [8] demonstrated that PVDF-based composite membrane with nano-sized ceramic powders could exhibit high proton conductivity when doped with some small molecular weight acid such as $H_2SO_4$. Panero et al. [9] prepared PVDF-based PEMs by swelling a silica-added PVDF membrane in a $H_3PO_4$ aqueous solution. They also demonstrated the critical role of dispersed ceramic fillers in controlling the methanol permeation. But the acid solution tends to migrate during the storage or at high temperature [9,10].

In this work, based on the method of Peled et al. [8] to prepare PVDF-based composite membranes, we adopted a kind of polymer acid poly(2-acrylamido-2-methyl propylene sulfonic acid) (PAMPS) as the swelling acid, which has not been reported by other authors. PAMPS has been shown to have good chemical stability and a high proton conductivity [11]. It has been used

* Corresponding author. Tel.: +86 10 62794234; fax: +86 10 62794234.
*E-mail address:* qiuxp@mail.tsinghua.edu.cn (X. Qiu).

0378-7753/$ – see front matter © 2005 Elsevier B.V. All rights reserved.
doi:10.1016/j.jpowsour.2005.11.070

in many fields including the electrochemical field [12–15]. Its application can be found in electrochromic devices as a proton conducting gel [12], humidity sensor [13], etc. The copolymers of AMPS with other monomers are used as PEMs in fuel cells [14,15]. The role of the PAMPS in the membrane is discussed. We also investigated the effect of different contents of nano-sized alumina powders on the proton conductivity and methanol permeability of the composite membrane.

## 2. Experimental

### 2.1. Preparation of composite membrane

PVDF powder ($M_w$ = 900,000, ShangHai San Ai New Material Co. Ltd.), together with a ceramic powder ($Al_2O_3$, 30 nm, Zhoushan Mingri Nanometer Material Co. Ltd.) were dispersed in a solvent mixture composed of propylene carbonate (PC) and cyclopentanone (CP). The mixture was heated at 60 °C and stirred to obtain a viscous solution and was cast onto a clean glass plate. Upon drying at 80 °C for several hours, a flexible membrane was obtained, noted as the precursor membrane PVDF–$Al_2O_3$ (PA). The membrane was washed several times with deionized water and then immersed in the aqueous solution of PAMPS (prepared by spontaneous polymerization of AMPS aqueous solution) (20 wt.%) at 90 °C. The resulted membrane was washed with deionized water to remove the remaining PAMPS. The final proton exchange membrane was denoted as PVDF–$Al_2O_3$–PAMPS (PAP). The thickness of the swelled membrane is about 200 μm. Membranes with different contents (*n* wt.%) of $Al_2O_3$ powders in the feed materials (PVDF + $Al_2O_3$) were prepared, denoted as PAP*n*. The alumina filler content, defined as the mass ratio $Al_2O_3$/(PVDF + $Al_2O_3$), varied from 5 to 75 wt.%. Its effect on the proton conductivity and methanol permeation performances of the final membrane is investigated. PVDF and PVDF–PAMPS membranes were also prepared for comparison in the similar way of PVDF–$Al_2O_3$ and PVDF–$Al_2O_3$–PAMPS membrane except for the addition of $Al_2O_3$ nano-powder.

### 2.2. Structural characterization

Infrared spectra (IR) were recorded on an AV360 infrared spectrophotometer with an ATR (attenuated total reflection) crystal over the range from 4000 to 700 $cm^{-1}$. The thermal stability of the membranes was studied by thermogravimetric analysis (TGA). The samples were heated from 40 to 500 °C at a rate of 20 °C $min^{-1}$ under a dry nitrogen atmosphere on Universal V5.3C TA Instrument, fitted with a TGA 2050 thermogravimetric thermal analyzer. The surface morphology of the composite membranes was observed on a scanning electron microscope (SEM, KYKY-2800).

### 2.3. Water uptake

Water uptake is defined by $W_{wet} - W_{dry}$, where $W_{dry}$ is the weight of the sample membrane dried in a vacuum oven under 100 °C for 12 h and $W_{wet}$ is the weight of the sample membrane saturated with distilled water for 48 h and weighed immediately after removing surface water with filtration paper.

### 2.4. Measurement of conductivity

Conductivity was measured using the ac impedance technology. The sample of the given swollen membrane was sandwiched between two stainless steel (SS) electrodes. A spring-loaded Teflon plunger was used to ensure an intimate contact between the end of the probe and the membrane of interest. The impedance tests were carried out in 1 MHz–1 Hz frequency range using a Solartron 1255B Impedance/Gain-Phase Analyzer coupled with a Solartron 1287 Electrochemical Interface.

### 2.5. Methanol permeability

A two-reservoir cell was used for the measurement of methanol permeability [16]. The left reservoir was filled with an aqueous solution of methanol (30 wt.%) while the right reservoir was filled with deionized water. The two reservoirs had a circularly symmetrical transport channel with the membranes separated between them. The methanol flux was established across the membrane driven by the concentration difference between the two reservoirs. The change of methanol concentration with time in the right reservoir was measured using a gas chromatographic instrument (Shimadzu, GC-14C).

## 3. Results and discussion

The structure of the PVDF–$Al_2O_3$ and PVDF–$Al_2O_3$–PAMPS membranes were characterized by FT-IR spectra and is shown in Fig. 1. There are three more bands in the spectra of the PVDF–$Al_2O_3$–PAMPS membrane than in the PVDF–$Al_2O_3$ membrane. The 3410 $cm^{-1}$ band is due to the stretching vibration of –NH– in the PAMPS. The 1641 $cm^{-1}$ band is due to the bending vibration of amide group in the PAMPS. The band of 1040 $cm^{-1}$ is the characteristic absorption peak of AMPS unit due to the SO group [12,17]. These all show the absorption of PAMPS in the final membrane.

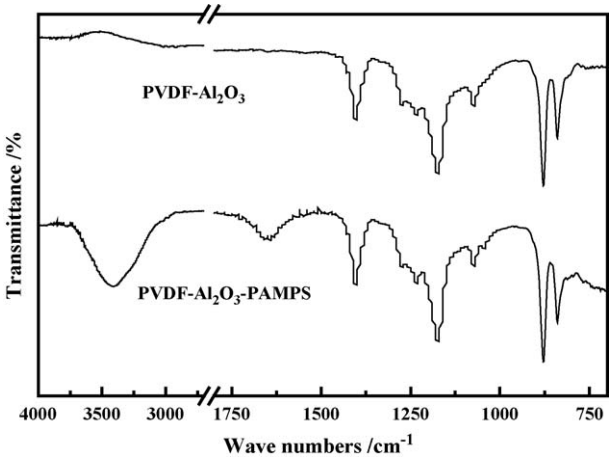


Fig. 1. FT-IR spectra of PVDF–$Al_2O_3$ and PVDF–$Al_2O_3$–PAMPS membrane.

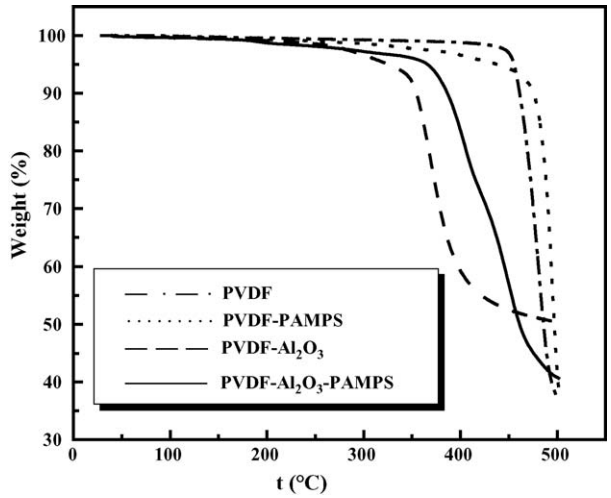


Fig. 2. TGA curves of PVDF, PVDF–PAMPS, PVDF–$Al_2O_3$ (5 wt.% of alumina), and PVDF–$Al_2O_3$–PAMPS (16 wt.% of alumina) membrane.

Fig. 2 shows the TGA curves of four membranes, PVDF, PVDF–PAMPS, PVDF–$Al_2O_3$, and PVDF–$Al_2O_3$–PAMPS. All the membranes lost less than 5% weight at temperature lower than 300 °C, which means although functional groups may be lost the framework of the PVDF-based membranes does not degrade until around 300 °C. Compared with the PVDF membrane, the PVDF–PAMPS membrane began to lose weight at a lower temperature of about 300 °C, corresponding to the decomposition of PAMPS. In contrast, the PVDF decomposition began at a higher temperature of about 470 °C, meaning the doping of the polymer acid helps to increase the thermal stability of the membrane rather than decrease it as the inorganic acids do [9,18]. This could also be found by comparing the membranes of PVDF–$Al_2O_3$ and PVDF–$Al_2O_3$–PAMPS. The role of the PAMPS is not only a proton donor but also a polymer matrix and does not have the problem of solution release. Although the addition of $Al_2O_3$ in the PVDF caused the membrane to decompose at 250 °C and made it less stable at high temperature, the thermal stability of the membrane is good enough to serve as a PEM in a DMFC.

Fig. 3 shows the surface SEM photographs of membrane PVDF, PVDF–$Al_2O_3$, and PVDF–$Al_2O_3$–PAMPS. The surface of PVDF membrane (Fig. 3a) is dense and homogeneous. When alumina powders were added, the membrane became less uniform as the alumina may aggregate to form small clusters (Fig. 3b). After swelling in PAMPS solution, the clusters became more dispersed (Fig. 3c). With the increase of alumina content, the membrane present a more crystalline aspect and the fillers tend to aggregate (Fig. 3d). If the content of alumina is increased to 75 wt.%, the membrane shows a rougher surface with a continuous phase of alumina and is flexible, more like a gel when exposed to water (Fig. 3e).

Table 1
Conductivities of PA16, PVDF–PAMPS, PAP16 membranes at room temperature

| Sample | $\sigma$ (S cm$^{-1}$) |
|---|---|
| PVDF–$Al_2O_3$ | $1.41 \times 10^{-4}$ |
| PVDF–PAMPS | $4.88 \times 10^{-3}$ |
| PVDF–$Al_2O_3$–PAMPS | $1.39 \times 10^{-2}$ |

We used the method of two electrodes ac impedance to measure the conductivities of the PVDF–$Al_2O_3$–PAMPS, PVDF–PAMPS, and PVDF–$Al_2O_3$ membranes. Their conductivities at room temperature are listed in Table 1. And the conductivity of the PVDF–$Al_2O_3$–PAMPS membrane restored in water is stable for 60 days at least.

Fig. 4 shows the water uptake and conductivities of PVDF–$Al_2O_3$–PAMPS (PAP) membranes related to the content of alumina initially added. The water uptake increases obviously with the increase of alumina content. It increases from 120% to about 370% when the content of alumina increases from 5 to 75%. The conductivity also increases with the increase of alumina contents (see Table 2). These demonstrate the importance of both $Al_2O_3$ and PAMPS to increase the conductivity of the PVDF–$Al_2O_3$–PAMPS membrane. The alumina powders as dispersed ceramic fillers help promote the liquid retention in the membrane due to their properties of hydrophillicity. A similar effect of acidic fillers in perfluorosulfonic membranes has been reported [19]. It has been shown that the filler absorbs water on the surface through a strong interaction with surface –OH groups and formation of hydrogen bonds, thus increasing the water retention and proton conductivity. Therefore, more alumina fillers promote the proton conductivity and modify the morphology of the membrane (Fig. 3a–e). It is the hydrophilicity of the alumina particles that allows PAMPS aqueous solutions to be inserted into an otherwise hydrophobic polymer matrix in the same way as $H_2SO_4$ or $H_3PO_4$ [18]. The PAMPS replaced the solvent of PC in the initial membrane during the swelling process and provides protons to transport in the membrane. It may be observed that the conductivities of the PVDF–$Al_2O_3$–PAMPS membranes are not as high as those of PVDF–HFP/$H_2SO_4$/$SiO_2$ or PVDF–HFP/$H_3PO_4$/$SiO_2$ membranes in literatures [9,18], due to the weaker dissociation of PAMPS and the more difficult absorption of macromolecules. But it is compensative the PVDF–$Al_2O_3$–PAMPS membranes are stable in the chemical components and in the proton conductivities upon heating and stored in water for 60 days. As shown in Fig. 3, the soak of PAMPS also helps alumina fillers disperse better in the membrane, and is supposed to act as a bridge to connect PVDF (with its hydrophobic matrix) and alumina segment (with its

Table 2
Proton conductivities ($\sigma$) and permeabilities ($P$) at room temperature of the PAP and Nafion 117 membranes

| | Pap5 | Pap16 | Pap50 | Pap75 | Nafion 117 |
|---|---|---|---|---|---|
| $\sigma$ (S cm$^{-1}$) ($T$ = 25 °C) | $5.52 \times 10^{-3}$ | $1.19 \times 10^{-2}$ | $1.69 \times 10^{-2}$ | $2.00 \times 10^{-2}$ | $3.33 \times 10^{-2}$ |
| $P$ ($\times 10^5$ cm$^2$ min$^{-1}$) | 5.432 | 2.603 | 3.366 | 3.614 | 7.091 |

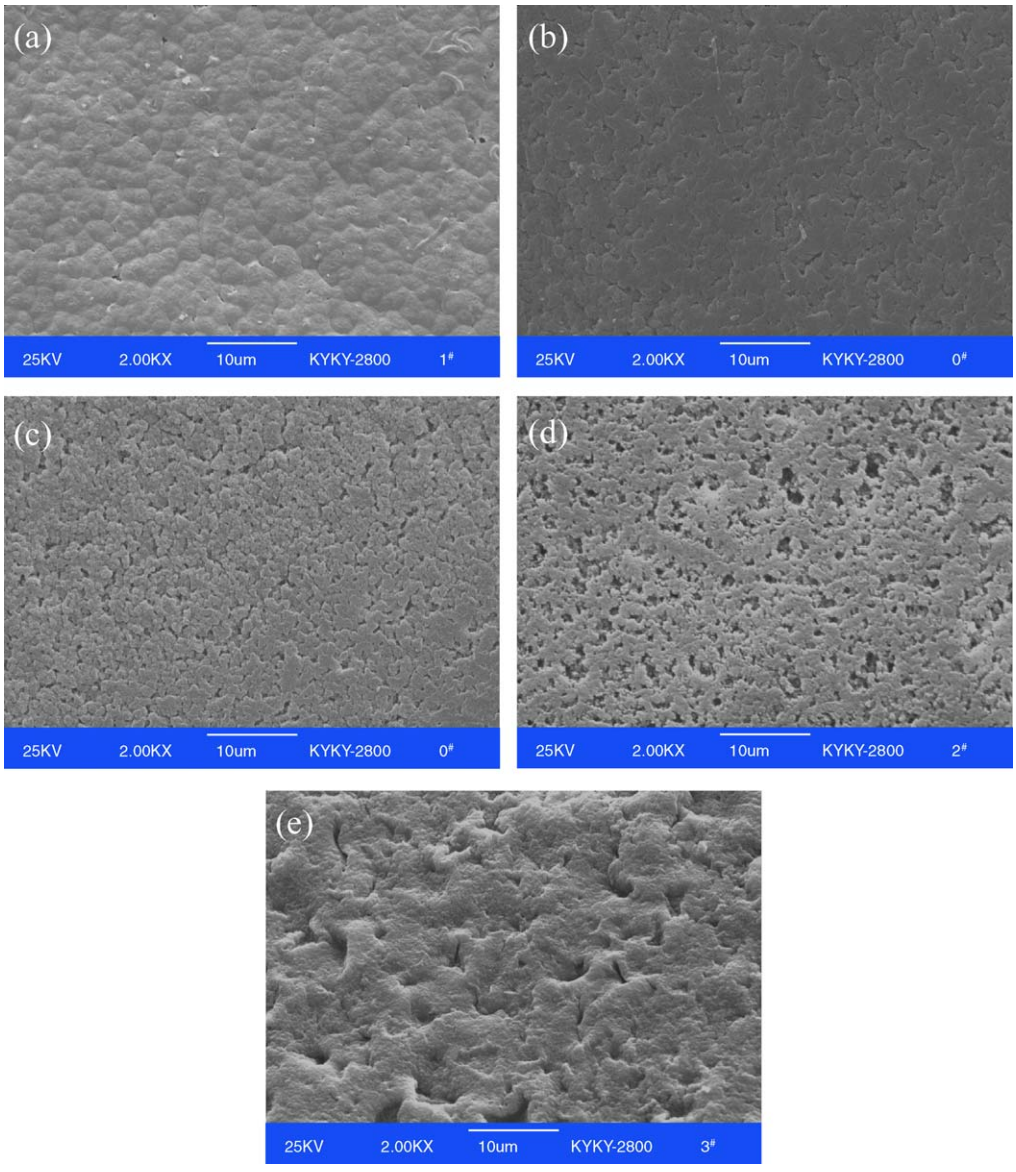


Fig. 3. Surface SEM photographs of membrane PVDF (a), PVDF–$Al_2O_3$ (5 wt.% of alumina) (b), and PVDF–$Al_2O_3$–PAMPS with 5 wt.% (c), 16 wt.% (d), and 75 wt.% (e) of alumina (scale bar: 10 μm).

hydrophilic sulfonic acid group). Moreover, as a polymer acid, the PAMPS could be retained in the membrane in the state of a gel or matrix, which does not release as do other monomeric inorganic acids (e.g. $H_2SO_4$ and $H_3PO_4$) (see FT-IR and TGA analyses above). This is the reason for the stability of the membrane.

Fig. 5 shows the proton conductivity change of PAP16 membrane in relation to the temperature. The conductivity of PVDF–$Al_2O_3$–PAMPS membrane reaches $1.4 \times 10^{-2}$ S cm$^{-1}$ at room temperature, which is comparable to that of Nafion 117. The conductivity of the membrane increases linearly with temperature ranging from 30 to 90 °C. According to the Arrhenius equation, the conductivity activation energy is 3.57 kJ/mol, indicating a little change with temperature.

We used a device described in Section 2 to measure the methanol permeation of membranes [16]. In this test, it is assumed that the change of the methanol concentration in the

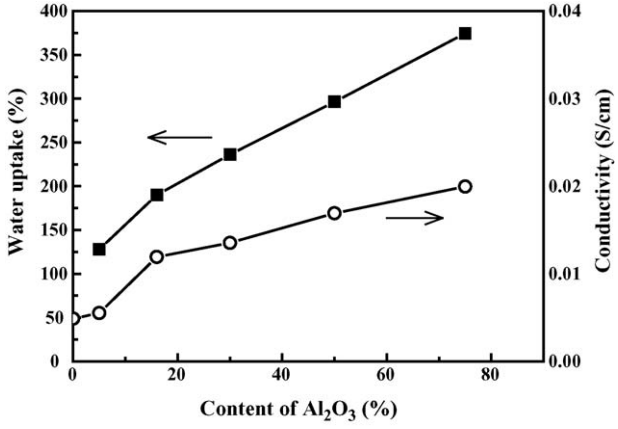


Fig. 4. Water uptake and conductivity of PVDF–$Al_2O_3$–PAMPS membranes with different contents of $Al_2O_3$.

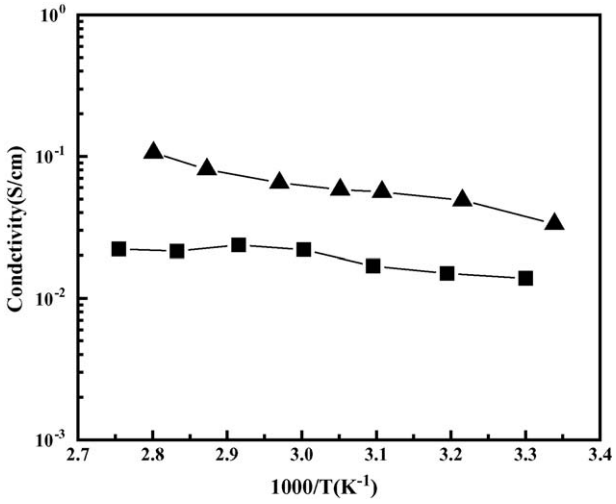


Fig. 5. Proton conductivity of PAP16 membrane (■) and Nafion 117 membrane (▲) in relation to the temperature.

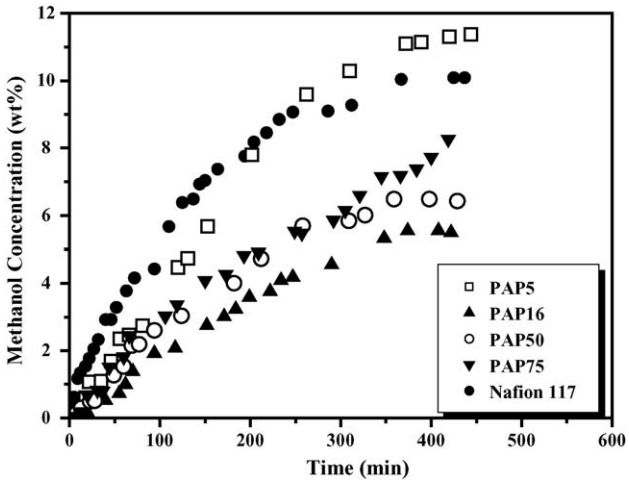


Fig. 6. Methanol concentration in the right reservoir ($c_B$) in relation to time during methanol permeation through PAP membranes and Nafion 117.

source side is negligible when the methanol concentration in the receiving reservoir is low. There is a pseudo-steady-state condition prevailing in the two reservoirs during the initial part of the experiment [20]. Accordingly, the flux of methanol is constant; the relationship of the methanol concentration in the receiving reservoir with time is given by:

$$V_B \frac{dc_B(t)}{dt} = A\frac{DK}{L}(c_A - c_B(t)) \quad (1)$$

where $c_A$ and $c_B$ are the methanol concentration in the left and the right reservoir, $A$ and $L$, the area and thickness of the membrane, $D$ and $K$, the methanol diffusivity and partition coefficient between the membrane and the adjacent solution, and $V_B$ is the volume of the right reservoir, respectively. The assumption that $D$ and $K$ are independent of the methanol concentration at the beginning of the experiment is made here. Eq. (1) can be solved to give:

$$V_B \ln\left[1 - \frac{c_B(t)}{c_A}\right] = -\frac{PA}{L}(t - t_0) \quad (2)$$

$P$ is the membrane permeability, defined as the product $DK$ and $t_0$ is the time lag.

Fig. 6 shows the relationship of the methanol concentration in the right reservoir (permeation side) with time using membranes of PAP series and Nafion 117. The linear behavior expected by Eq. (2) is observed in Fig. 7 and $P$ can be obtained from the slopes of the straight lines. The permeabilities, together with conductivities, of the membranes are listed in Table 2. We can observe from these values that these PVDF-based composite membranes have lower permeabilities than Nafion 117. The increase in alumina content causes changes in the methanol permeability. The permeability decreased by more than a half when the alumina content increased from 5 to 16%. This was also observed in the case of Nafion/silica hybrid membranes [3,4] and PVA/zeolite composite membranes with low content of ceramic fillers [7]. But if the alumina content increased to 50 and 75%, the permeability would become higher than that in the case of 16%, but still lower than that of 5%. This can be explained from the phase-separated structure of the membrane. With a low filler loading, the alumina particles are separated by polymer matrix and methanol could pass through pathways formed by hydrophilic part of PAMPS. When the filler loading is increased to an extent (e.g. 16 wt.%), they are dispersed in the polymer matrix and could be obstacles in the pathway of methanol. At high loading (over 50 wt.%), the alumina particles tend to aggregate to larger clusters and become continuum. Methanol could easily go through porous channels formed by the large clusters [9]. From the results of this work, we found the transport mechanisms of proton and methanol are different in the case of the PVDF composite membrane with ceramic fillers and PAMPS. It is assumed the protons shuttled through the alumina fillers while the methanol goes around the alumina fillers, as described in literature [7].

The ideal PEM for a DMFC is expected to have high proton conductivity and low methanol permeability. The ratio between proton conductivity to methanol permeability in the membrane, $\Phi$, is used here to describe the membrane performance. The

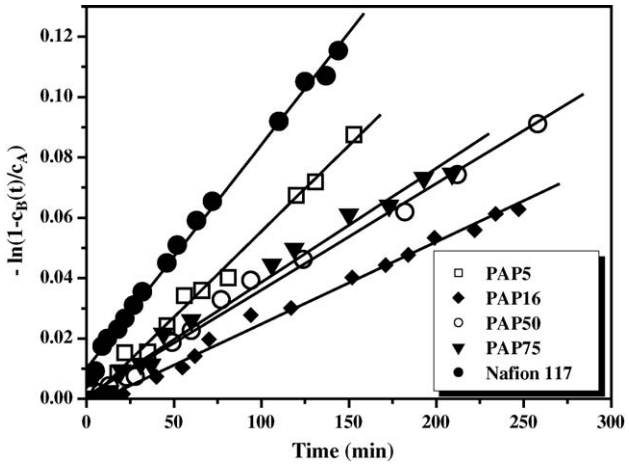


Fig. 7. $-\ln(1 - c_B/c_A)$ vs. time of methanol permeated through PAP and Nafion 117 membranes.

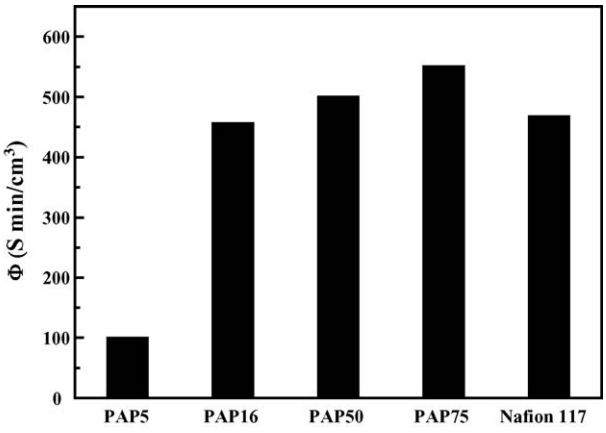


Fig. 8. Proton conductivity/methanol permeability, $\Phi$, for PAP series and Nafion 117 membranes.

higher $\Phi$ value, the better the membrane performance. The $\Phi$ values of membranes investigated in this work are compared in Fig. 8. We can infer from it that the PAP membranes with more alumina fillers (greater than 16 wt.%) would perform better in the DMFC than with fewer alumina fillers (5 wt.%). The $\Phi$ value of PAP16 membrane is close to that of Nafion 117, and the value of PAP50 and PAP75 is higher than that of Nafion 117.

## 4. Conclusions

The PVDF-based composite PEM was prepared by addition of ceramic powders and doping of PAMPS. The roles of the alumina fillers and the PAMPS in the PEM are discussed. Use of a polymeric water-insoluble ionomer, like PAMPS, in the membrane solved the problem of ionomer loss from the membrane and made it applicable in a DMFC. This composite membrane shows high thermal stability, high conductivity at room temperature and low methanol permeability. The water uptake and proton conductivity increased with the content of alumina filler. Methanol permeation is reduced with high alumina filler content. The membranes with high alumina filler contents are promising for use in the DMFC due to their high $\Phi$ values. Further investigations are in progress to apply these PVDF-based composite membranes to DMFC operation.

## Acknowledgements

This work was financially supported by the State Key Basic Research Program of China (2002CB211803). J. Xi thanks the China Postdoctoral Science Foundation for financial support.

## References

[1] X.M. Ren, T.E. Springer, T.A. Zawodzinski, S. Gottesfeld, J. Electrochem. Soc. 147 (2000) 466.
[2] T.A. Zawodzinski, M. Neeman, L.O. Sillerud, S. Gottesfeld, J. Phys. Chem. 95 (1991) 6040.
[3] N. Miyake, J.S. Wainright, R.F. Savinell, J. Electrochem. Soc. 148 (2001) A905.
[4] D.H. Jung, S.Y. Cho, D.H. Peck, D.R. Shin, J.S. Kim, J. Power Sources 106 (2002) 173.
[5] V. Tricoli, F. Nannetti, Electrochim. Acta 48 (2003) 2625.
[6] Z. Połtarzewski, W. Wieczorek, J. Przyłuski, V. Antonucci, Solid State Ionics 119 (1999) 301.
[7] B. Libby, W.H. Smyrl, E.L. Cussler, Electrochem. Solid-State Lett. 4 (2001) A197.
[8] E. Peled, T. Duvdevani, A. Melman, Electrochem. Solid-State Lett. 1 (1998) 210.
[9] S. Panero, F. Ciuffa, A. D'Epifano, B. Scrosati, Electrochim. Acta 48 (2003) 2009.
[10] M.A. Navarra, S. Materazzi, S. Panero, B. Scrosati, J. Electrochem. Soc. 150 (2003) A1528.
[11] J.P. Gong, N. Komatsu, T. Nitta, Y. Osada, J. Phys. Chem. B 101 (1997) 740.
[12] G. Zukowska, J. Williams, J.R. Stevens, K.R. Jeffrey, A. Lewera, P.J. Kulesza, Solid State Ionics 167 (2004) 123.
[13] P.G. Su, W.Y. Tsai, Sens. Actuators B 100 (2004) 425.
[14] C.W. Walker Jr., J. Power Sources 110 (2002) 144.
[15] L.E. Karlsson, B. Wesslen, P. Jannasch, Electrochim. Acta 47 (2002) 3269.
[16] X.P. Qiu, W.Q. Li, S.C. Zhang, H.Y. Liang, W.T. Zhu, J. Electrochem. Soc. 150 (2003) A917.
[17] S. Durmaz, O. Okay, Polymer 41 (2000) 3693.
[18] J.C. Lassegues, J. Grondin, M. Hernandez, B. Maree, Solid State Ionics 145 (2001) 37.
[19] A.S. Arico, V. Baglio, A. Di Blasi, V. Antoncci, Electrochem. Commun. 5 (2003) 862.
[20] V. Tricoli, J. Electrochem. Soc. 145 (1998) 3798.